Temporal characteristic simulation for stimulated emission depletion microscopy

Wenxia Chen (陈文霞), Fanrong Xiao (肖繁荣), Li Liu (刘 力), and Guiying Wang (王桂英)

State Key Laboratory of High Field Laser Physics, Shanghai Institute of Optics and Fine Mechanics, Chinese Academy of Sciences, Shanghai 201800

The imaging technology of stimulated emission depletion (STED) utilizes the nonlinearity relationship between the fluorescence saturation and the excited state stimulated depletion. It implements three-dimensional (3D) imaging and breaks the diffraction barrier of far-field light microscopy by restricting fluorescent molecules at a sub-diffraction spot. In order to improve the resolution which attained by this technology, the computer simulation on temporal behavior of population probabilities of the sample was made in this paper, and the optimized parameters such as intensity, duration and delay time of the STED pulse were given.

OCIS codes: 110.0180, 180.2520, 180.6900, 190.7110, 260.3060.

Far-field fluorescence light microscopy is a main technique for investigating and detecting biological specimens, because the focused beams can penetrate high scatter media with the intention of imaging living specimens with three-dimensional (3D). But its resolution is limited by the diffraction barrier[1] which depends on the smallest focusing light spot size.

The diffraction barrier and limited resolution in far-field fluorescence microscopy has been fundamentally broken by utilizing the nonlinearity relationship between the fluorescence saturation and the excited state stimulated depletion, which called stimulated emission depletion (STED). It is reported that Hell team have attained spots of 33-nm width along the optic axis [2] and lateral resolution of 28 nm, which corresponding to 1/25 of wavelength[3]. This improvement is obtained by quenching the excited fluorescence at the out part of the excitation focal spot with a beam whose wavelength is at the red edge of the fluorescent emission spectrum. Consequently the remaining fluorescence stems from a region that is narrower than the diffraction-limited size.

There are two kinds issues in the STED fluorescence microscopy, one is the spatial shaping of the stimulating beam, so as to render a focal spot with a central hole; the other is the spectroscopy and aims at realizing a set of conditions that enables the complete depletion of the excited state by stimulated emission.

In theory, the ideal focal intensity distribution of the STED pulse should subject to the function[4] $I_{\mathrm{STED}}(\vec{r},t) = \begin{cases} 0, & \text{for } \vec{r}=0 \\ \gg 0, & \text{else} \end{cases}$, which ensures that the center of the fluorescence spot is spared out from depletion, whereas its periphery there the fluorescent molecules are strongly depleted. Therefore only molecules, which happen to be close to the focal point, contribute to the detected signal, so theoretically the achievable spatial resolution is on a molecular scale. But in practice it is limited by the finite depth of the central minimum formed by the molecules, and the resolution will be further increased if larger depletion efficiency can be attained. So the computer simulation on the temporal behaviors of population probabilities of the sample was made in this paper, and the optimized parameters such as intensity, duration, and delay time of the STED pulse were given to improve the depletion efficiency.

Meeting the spectroscopic conditions is based on the fact that actually all fluorophores are four-level systems. Taking this into account, the energy levers involved in the excitation and the subsequent emission process of a typical fluorophore was displayed in Fig. 1[5].

After its excitation to a higher vibrational level L_1 of the first excited electronic state S_1, the molecules nonradiatively decay to the low-lying fluorescent state L_2. The red shifted depletion pulse induces stimulated emission in L_2 and pushes the molecules to a higher vibrational level L_3 of the ground state S_0, which decays to the low vibrational level L_0.

The temporal behaviors of the population probabilities n_i (t) of levels L_i $(i = 0,1,2,3)$ of the dye can be described by a set of coupled differential equations, relating the interplay among absorption, quenching, vibrational relaxation, stimulated emission, and spontaneous emission[4,5]:

$$\frac{\mathrm{d}n_0}{\mathrm{d}t} = \frac{I_{\mathrm{exc}}\sigma_{01}(n_1 - n_0)}{h\nu_{\mathrm{exc}}} + \frac{1}{\tau_{\mathrm{vibr}}}n_3, \tag{1}$$

$$\frac{\mathrm{d}n_1}{\mathrm{d}t} = \frac{I_{\mathrm{exc}}\sigma_{01}(n_0 - n_1)}{h\nu_{\mathrm{exc}}} - \frac{1}{\tau_{\mathrm{vibr}}}n_1, \tag{2}$$

$$\frac{\mathrm{d}n_2}{\mathrm{d}t} = \frac{I_{\mathrm{STED}}\sigma_{23}(n_3 - n_2)}{h\nu_{\mathrm{STED}}} + \frac{1}{\tau_{\mathrm{vibr}}}n_1 - (\frac{1}{\tau_{\mathrm{fluor}}} + Q)n_2, \tag{3}$$

$$\frac{\mathrm{d}n_3}{\mathrm{d}t} = \frac{I_{\mathrm{STED}}\sigma_{23}(n_2 - n_3)}{h\nu_{\mathrm{STED}}} - \frac{1}{\tau_{\mathrm{vibr}}}n_3 + (\frac{1}{\tau_{\mathrm{fluor}}} + Q)n_2, \tag{4}$$

$$\sum\nolimits_i n_i = 1, \tag{5}$$

$$n_0(t=0) = 1, \tag{6}$$

where Q is the quenching rate, τ_{fluor} and τ_{vibr} are the average fluorescence lifetime and vibrational relaxation

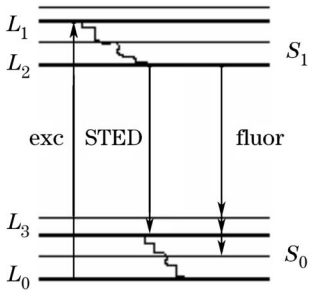

Fig. 1. Energy levels of a typical fluorophore.

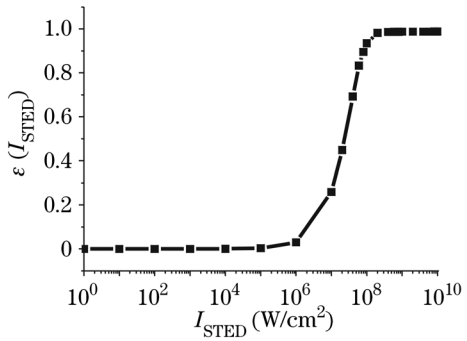

Fig. 2. Time-averaged depletion efficiency as a function of $I_{\rm STED}$.

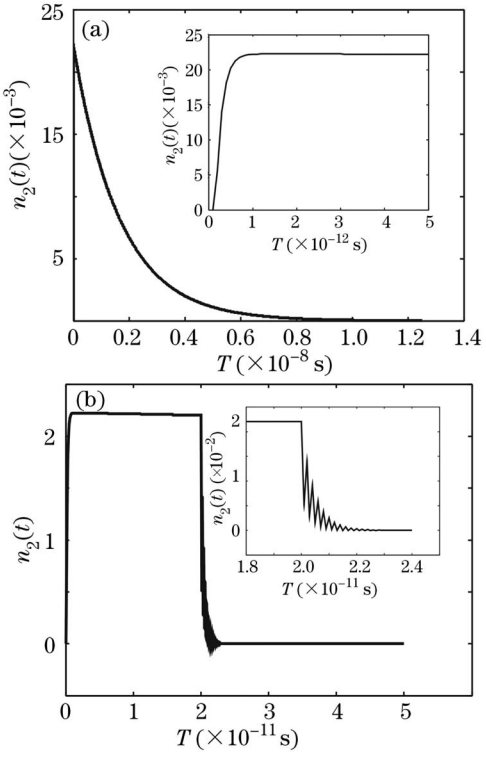

Fig. 3. Temporal behaviors of population probabilities n_2, with $I_{\rm STED} = 0$(a) and $I_{\rm STED} = 10^{10}$ W/cm^2 (b).

time; σ_{01} and σ_{23} are the molecular cross-section for the transition $L_0 \leftrightarrow L_1$ and $L_2 \leftrightarrow L_3$; $h\nu_{\rm exc}$ and $h\nu_{\rm STED}$ are the photon energies and $I_{\rm exc}$ and $I_{\rm STED}$ are the local intensities of excitation and STED beams, respectively. $\frac{I_{\rm exc}\sigma_{01}(n_1-n_0)}{h\nu_{\rm exc}}$ describes the absorption and emission from L_1 and L_2 by excitation beam, $\frac{I_{\rm STED}\sigma_{23}(n_3-n_2)}{h\nu_{\rm STED}}$ describes the stimulated emission from L_2 and re-excitation from L_3 by stimulating beam, and $(\frac{1}{\tau_{\rm fluor}}+Q)n_2$ describes the decay of n_2 by spontaneous emission and quenching. Equations (5) and (6) denote the normalized probabilities for the total population and the initialization.

To simulate the temporal behaviors of n_i, some parameters of the coupled differential equations are set as follow: $\sigma_{01} = 4\times10^{-16}$ cm^2, $\sigma_{23} = 2\times10^{-16}$ cm^2, $\tau_{\rm fluor} = 2\times10^{-9}$ s, $\tau_{\rm vibr} = 0.2\times10^{-12}$ s, $Q = 10^8$ s^{-1}, $\lambda_{\rm exc} = 560\times10^{-9}$ m, $\lambda_{\rm exc} = 765\times10^{-9}$ m. Here the fluorescence wavelengths range from 650 to 800 nm[6]. The excitation and STED pulses are supposed as rectangular pulses and their mathematic expressions are given as $I_{\rm exc}(t) = \begin{cases} I_0^{\rm exc}, & {\rm for} 0\le t\le\tau_{\rm exc} \\ 0, & {\rm else}\end{cases}$ and $I_{\rm STED}(t) = \begin{cases} I_0^{\rm STED}\cdots{\rm for}\cdots 0\le t\le\tau_{\rm STED} \\ 0\cdots\cdots{\rm else}\end{cases}$, $\tau_{\rm exc}$ and $\tau_{\rm STED}$ refer to the duration time of excitation and STED pulses, respectively. Delay time Δt denotes the time between the climbing-edge of excitation and STED pulses.

Only to demonstrate that the temporal behaviors of n_i is not enough, so we also simulate the time-averaged depletion efficiency ε of the fluorescent state, which is defined as $\varepsilon = \varepsilon(I_{\rm STED}) = 1 - \frac{\int_0^T n_2(t, I_{\rm STED}(t))\,{\rm d}t}{\int_0^T n_2(t,0)\,{\rm d}t}$, T is the integral time, which is set as the interval time of pluses train here.

Firstly, the nonlinear relationship between STED intensity and time-averaged depletion efficiency of the fluorescent state are demonstrated in Fig. 2. $I_{\rm STED}$ varies from 0 to 10^{10} W/cm^2 and other parameters are selected as follow: $I_{\rm exc} = 10^8$ W/cm^2, $\tau_{\rm exc} = 0.2\times10^{-12}$ s, $\tau_{\rm STED} = 40\times10^{-12}$ s, $\Delta t = 20\times10^{-12}$ s. Figure 2 shows that when $I_{\rm STED}\le 10^6$W/cm^2, the time-averaged depletion efficiency ε is almost not change and approximates to 0; when $10^6\le I_{\rm STED}\le 2\times10^8$ W/cm^2, with intensity increasing, ε increases sharply, and changes from 0.03 to 0.9820; with $I_{\rm STED}$ continuing increasing, ε is approaching saturation and close to 100%. We can conclude that when $I_{\rm STED}\le 10^6$ W/cm^2 which may be named as "threshold intensity", or $I_{\rm STED}\ge 2\times10^8$ W/cm^2, the temporal behaviors of the population probabilities n_2 are almost of the same, respectively. Contrastively, when $I_{\rm STED}$ at the range of $10^6\le I_{\rm STED}\le 2\times10^8$ W/cm^2, the temporal behaviors of n_2 depend on $I_{\rm STED}$ acutely. Consequent we will analysis the temporal behaviors of n_2 at different typical intensities.

Observing Fig. 3, at the initial time, the fluorescent state is empty. After 0.2 ps, particles begin to occupy L_2 and the population adds, at about 1 ps the population reaches its maximum. Then if $I_{\rm STED}$ is low enough as to render the rates of the stimulated transition much slower than $1/\tau_{\rm vibr}$, re-excitation is negligible, and the vibrational state near empty, so $n_1\approx 0$, $n_3\approx 0$. Hence, the population of the fluorescent state and the remaining fluorescence obeys the proportionality $n_2(t)\propto\exp[-(\frac{1}{\tau_{\rm fluor}}+Q)t]$ in good approximation, this means that n_2 is governed by the fluorescence emission rate. But for higher intensity, after the population reached the maximum, it keeps constant during the

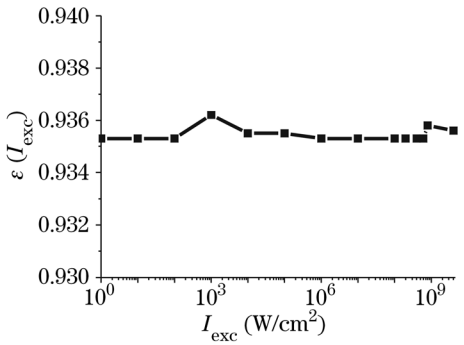

Fig. 4. Time-averaged depletion efficiency as a function of $I_{\rm exc}$.

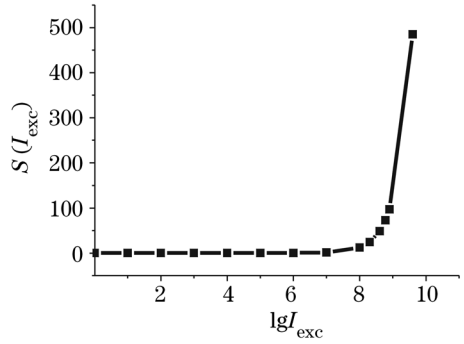

Fig. 5. The sum of n_2 as a function the excitation intensity $I_{\rm exc}$.

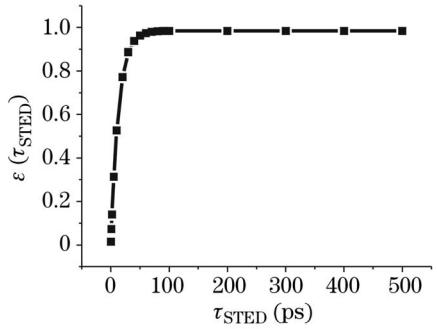

Fig. 6. Time-averaged depletion efficiency as a function of $\tau_{\rm STED}$.

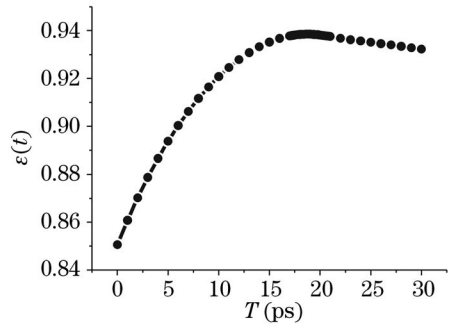

Fig. 7. Time-averaged depletion efficiency as a function of the delay time Δt.

delay time, when STED pulse begins to operate, n_2 decays faster than the low intensity case, and as the whole procession it is determined by the fast vibrational relaxation but with damping oscillation. For the condition that $10^6 \leq I_{\rm STED} \leq 2\times10^8$ W/cm^2, the temporal behavior of n_2 depends on $I_{\rm STED}$ and the decay time changes from $\tau_{\rm fluor}$ to $\tau_{\rm vibr}$, because all influence of fluorescence emission, quenching, STED intensity, and vibrational relaxation cannot be neglected. Moreover, since σ_{23} plays the same role of $I_{\rm STED}$ in Eq. (3), we can select samples with big σ_{23} to enhance the depletion efficiency.

Then the influence of $I_{\rm exc}$ to the depletion efficiency is considered. We Keep the intensity $I_{\rm STED} = 10^8$ W/cm^2, and change the value of $I_{\rm exc}$ from zero to 10^{10} W/cm^2. In Fig. 4, we can see that ε approximately keeps the same value. But when consider the sum of population probabilities of fluorescent state in a period interval which defined as $S(I_{\rm exc}) = \int_0^T n_2(t, I_{\rm exc}){\rm d}t$. In Fig. 5, we find that with $I_{\rm exc}$ increasing, the total signal $S(I_{\rm exc})$ increases by degrees, but when $I_{\rm exc} \leq 10^7$ W/cm^2, it nears zero and are too small to demonstrate its different values in the picture, if $I_{\rm exc} \geq 10^7$ W/cm^2, it adds sharply. Therefore, though $I_{\rm exc}$ almost does not influnce the depletion efficiency, while considering about other background light in the experiment, in order to improve the signal-to-noise ratio, the detected signal is better to be bigger, so we had better to set $I_{\rm exc}$ with bigger value.

When investigate the duration of excitation pulse, we get the conclusion that increasing the pulse duration is equal to increasing the intensity, because increasing either the duration or intensity, it all adds the population of the photons per pulse, and it means more photons are pumped then down to the fluorescent state.

Next we let $\tau_{\rm STED}$ increases from 0.2 to 500 ps, and keep $I_{\rm STED} = 10^8$ W/cm^2, change $\tau_{\rm exc}$ into 20 ps to distinguish the influence of $\tau_{\rm exc}$ and $\tau_{\rm vibr}$. The numerical results are described as the curve of the time-averaged depletion efficiency as a function of $\tau_{\rm STED}$ in Fig 6. In which the curve climbs fast at the beginning, and then rise slowly, when $\tau_{\rm STED} \geq 200$ ps, it becomes a constant. Comparing Figs.6 and 2, the two curves almost move in the same rule, that means that increasing the duration is equal to increasing the intensity, for the reason that they all adds the population of the photons per pulse.

Since the typical life time of the fluorescent state is about 1–5 ns, STED pulse has to be completed within a fraction of this time. This condition gives an upper limit of approximately 200–1000 ps for the duration of STED pulse. Conversely, there is a lower limit of approximately 1–2 ps which stems from the fact that transient filling of the higher vibrational level of the ground state must be avoided[7].

Then we study the key parameter: the delay time Δt, which refers to the time that STED pulse after the excitation pulse, the accurate definition is given above. We set $\tau_{\rm exc} = 20\times10^{-12}$ s, $\tau_{\rm STED} = 40\times10^{-12}$ s, others keep the same values, and add Δt from 0 to 30 ps step by step, around the maximum, we insert some points with 0.2-ps interval which equal to $\tau_{\rm vibr}$ to see about whether $\tau_{\rm vibr}$ has some infection on the depletion efficiency.

From Fig. 7, we can see that with the increasing of the delay time, ε becomes bigger, when 17.4 (ps) $\leq \Delta t \leq$ 20.2 (ps) which is be close to the duration of the excitation

pulse, ε is larger than 0.938, and at 18.8 ps , it gets to the maximum, then with bigger delay time, it declines slowly. We can conclude that the optimal value of Δt is such that the STED pulse arrives as soon as the excitation pulse is about to leave, which can be expressed as $\tau_{\rm exc} - 2.6$ (ps) $\leq \Delta t_{\rm opt} \leq \tau_{\rm exc} + 0.2$ (ps). In this case, within the restricted sub-diffraction spot, L_2 is almost not being populated while the fluorescence is radiating.

In conclusion, we have investigated the temporal behaviors of the population probabilities of the excited level of a material, and the relationships between the time-averaged depletion efficiency and the key parameters such as $I_{\rm exc}$, $\tau_{\rm exc}$, $I_{\rm STED}$, $\tau_{\rm STED}$, and Δt. We gain the rules as following: first, increasing $I_{\rm exc}$ and $\tau_{\rm exc}$ are equal to adds the photons per pulse of excitation beam, although they not to enhance efficiency directly, they increase the total signal; second, increasing $I_{\rm STED}$ and $\tau_{\rm STED}$ are equal to adds the photons per pulse of STED beam, and before their saturation, the bigger they are the higher efficiency it gets; third, when $\tau_{\rm exc} - 2.6$ (ps) $\leq \Delta t_{\rm opt} \leq \tau_{\rm exc} + 0.2$ (ps), STED light beam just reaches as soon as the excitation pulse is about to leave, it gets the maximum efficiency. In STED microscopy, the time size control is vital technique for improving the system resolution.

Through above simulation calculation and analysis, we expect the resolution can reach the molecule scale, and is able to image inside a 3D volume, due to its sectional function, and it could be implemented in standard cofocal beam scanners, also it can be combined with total internal reflection microscopy to create spatially controlled excitation profiles[8]. STED microscopy should play a more and more important role in the future.

This work was supported by National "973" Program of China (No. 2002CB713808) and National Natural Science Foundation of China (No. 60408007). W. Chen's e-mail address is wenxia@mail.siom.ac.cn.

References

1. E. Abbe, *Gesammelte Abhabdlungen* (G. Fischer, Jena, 1904).
2. Westphal, V. L. Kastrup, and S. W. Hell, Appl. Phys. B **77,** 377 (2003).
3. M. Dyba and S. W. Hell, Phys. Rev. Lett. **88,** 163901 (2003).
4. T. A. Klar, E. Engel, and S. W. Hell, Phys. Rev. E **64,** 066613 (2001).
5. S. W. Hell and J. Wichmann, Opt. Lett. **19,** 780 (1994).
6. T. A. Klar, S. Jakobs, M. Dyba, and S. W. Hell, PNAS, **97,** 8206 (2000).
7. M. Dyba and S. W. Hell, Appl. Opt. **42,** 5123 (2003).
8. G. E. Cragg and P. T. C. So, Opt. Lett. **25,** 46 (2000).